Copyright

by

Paola Anaid González Garza

2013

The Thesis Committee for Paola Anaid González Garza
Certifies that this is the approved version of the following thesis:

Effects of Nanoconfinement on Structure and Properties of Side-Chain Liquid Crystalline Polymers

APPROVED BY
SUPERVISING COMMITTEE:

Supervisor:

Christopher J. Ellison

C. Grant Willson

Effects of Nanoconfinement on Structure and Properties of Side-Chain Liquid Crystalline Polymers

by

Paola Anaid Gonzalez Garza, B.S.M.E.

Thesis

Presented to the Faculty of the Graduate School of

The University of Texas at Austin

in Partial Fulfillment

of the Requirements

for the Degree of

Master of Science in Engineering

The University of Texas at Austin

December 2013

Dedication

To my parents for their unconditional support.

Ma y Pa, ¡gracias! Sin ustedes no hubiera pasado del primer año.

And to the rest of my family; thank you for always being there when I needed you and for not abandoning me in the tough years.

Acknowledgements

I would like to thank Dr. C. Ellison for his invaluable time and patience during my time in lab, as well as Dr. G. Willson for his time in reviewing this thesis. Thank you to the Center for Layered Polymeric Systems (CLiPS) and the Consejo Nacional de Ciencia y Tecnologia (CONACYT) for their financial support of this research. A lot of the research presented here would not have been possible without the help of everyone in the Ellison research group, especially Dr. Dustin Janes, Dr. Sateesh Peddini, and Zhenpeng Li. Thank you as well to members of the Willson research group for their advice. I also need to thank Matthew Herbert for his help in editing and proofreading this work.

Abstract

Effects of Nanoconfinement on Structure and Properties of Side-Chain Liquid Crystalline Polymers

Paola Anaid González Garza, M.S.E.

The University of Texas at Austin, 2013

Supervisor: Christopher J. Ellison

Semi-crystalline polymers have shown increased crystalline order and size when confined in multilayered films by coextrusion[1]. The resulting large crystals lead to dramatic improvements in gas barrier properties. Ordered polymers whose characteristics are between that of the liquid phase and the crystalline phase are known as liquid crystalline polymers. The highly ordered mesogens in liquid crystalline polymers contribute to their exceptional bulk properties. In this research, side-chain liquid crystalline polymers were confined in multilayered films, made by either multilayer coextrusion or spin coating, with a non-liquid crystalline polymer in an attempt to improve the ordering of the liquid crystalline mesogens. The liquid crystalline behavior and morphology was studied to understand the correlation between the confinement size and the properties of the multilayer films. Commercial main chain liquid crystalline polymers and hydrogen

bonded liquid crystalline polymers were also explored in this research for their use in multilayer coextrusion.

Table of Contents

List of Tables

List of Figures

List of Abbreviations

ΔT_{LC}	Temperature range over which the mesophase occurs
D	Diffusivity
DCM	Dichloromethane
DPE	1,2-Di(4-pyridyl)ethylene
DSC	Differential Scanning Calorimetry
FT-IR	Fourier transform infrared spectroscopy
HBLCP	Hydrogen bonded liquid crystalline polymers
HIQ	Hydroxybenzoic acid / isophthalic acid / hydroquinone
^{1}H-NMR	Proton nuclear magnetic resonance
LC	Liquid crystal
LCI	Liquid crystal ionomer
LCP	Liquid crystal polymer
LCP_{NMe}	Side chain liquid crystalline polymer with tertiary amine end group
LCP_{OMe}	Side chain liquid crystalline polymer with methoxy end group
MCLCP	Main chain liquid crystalline polymer
MEK	Methyl ethyl ketone (2-Butanone)
MeOH	Methanol
OMe	Mesogen with hexamethylene flexible spacer and a methoxy end group
NMe	Mesogen with hexamethylene flexible spacer and a tertiary amine end group
P	Permeability
PBT	Polybutylene terephthalate

PC	Polycarbonate
PE-co-PAA	Poly(ethylene-co-acrylic acid)
PE-co-PMAA	Poly(ethylene-co-methacrylic acid)
PEN	Poly(ethylene-co-norbornene)
PET	Polyethylene terephthalate
PHOS	Poly(4-hydroxystyrene)
POM	Polarizable optical microscopy
PS	Polystyrene
PS-LCP_{NMe}-PS	Triblock composed of polystyrene and side chain liquid crystalline polymer with a hexamethylene spacer and tertiary amine end group
PS-LCP_{OMe}-PS	Triblock composed of polystyrene and side chain liquid crystalline polymer with a hexamethylene spacer and methoxy end group
PS-PHOS-PS	Triblock composed of polystyrene and poly(4-hydroxystyrene)
PS-PtBOS-PS	Triblock composed of polystyrene and poly(4-*tert*-butoxystyrene)
PVDF	Polyvinylidene fluoride
S	Solubility
S	Order parameter
SCLCP	Side chain liquid crystalline polymer
SEM	Scanning electron microscopy
T_c	Crystallization temperature
T_g	Glass transition temperature
T_{iso}	Isotropization temperature
T_m	Melting temperature
TGA	Thermogravimetric analysis
WAXD	Wide angle X-ray diffraction

Introduction

Liquid crystalline polymers (LCPs) have exceptional properties, such as high tensile strength, high thermal and chemical resistance, birefringence and low gas/liquid permeabilities. These features are a result of their ordered, rigid molecular substituents. They have captured the interest of materials researchers since their discovery in the 1930s due to potential in non-linear optics, ferroelectric, barrier, and information storage applications. For barrier applications, i.e. packaging and coatings, LCPs have been less successfully adopted due to the challenges associated with melt processing into films and the cost of these materials.

OBJECTIVE

Given the need for better performing materials, this research focused on obtaining thin films derived from liquid crystalline polymers (LCPs), which could be implemented in gas barrier applications. Since liquid crystalline polymers have already been shown to have low gas permeabilities in bulk, both from a decrease in gas solubility and diffusivity[2], this project seeks to further explore the possibility of using LCPs for this purpose, but in thin films. However, the viscosity of LCPs tend to be low with a very strong temperature dependence making them challenging to process into thin films for barrier applications. This coupled with the high cost of commercial LCPs, due to the often difficult synthetic procedure for making them, has prevented LCPs from being widely used. The proposed research targets multilayering as a strategy for manufacturing LCPs into high performance barrier films where the LCP is only a small fraction of the film. However, the processing challenge must be overcome. Additionally, this research will explore whether LCP layers have enhanced liquid crystallinity when confined to submicron thin films similar to what has been observed for confined crystallizable

polymers[1,3-6], as well as explore how any changes in ordering are linked to changes in their physical properties.

SIGNIFICANCE

LCPs have been considered materials with high potential due to their excellent chemical, mechanical, and optical properties. One of these properties in which LCPs outperform other polymers is gas barrier properties. However, because of the high cost of LCPs and the challenges present during melt-processing, their full potential has not yet had an impact in a wide array of markets. By incorporating LCPs into films with multiple layers it is expected that the LC properties will be conserved, or even enhanced, while the total quantity of LCP used is decreased, and thus the total cost of the polymer film is also reduced.

Although it is well known that many of the LCP properties of interest are directly affected by the ordering of the mesogens[7], studies of LCP ordering and how it affects its properties when confined to submicron thin films are scarce and often contradicting. The studies presented in this thesis provide insight in to how ordering is affected by confinement. This understanding will provide the ability to control the ordering during or after manufacturing of these films to obtain the desired physical properties.

Background

Liquid Crystalline Polymers

LCPs contain rigid, usually rod-like molecules with strong dipoles or polarizable substituents, called mesogens, attached to polymer chains either covalently or through non-covalent interactions. Initial interest in this type of polymer came from the mesogens' ability to align their individual molecule axis (shown in blue) along a common direction known as the assembly director (shown in grey) as seen in Figure 1b. The mesophase, the phase in which the mesogens are aligned, can be obtained by either changing the polymer temperature (thermotropic LCPs) or the concentration of mesogens in solution (lyotropic LCPs). This study is only concerned with thermotropic LCPs. Figure 1 shows the mesogen ordering structures in the crystalline, liquid crystalline and isotropic phases, respectively.

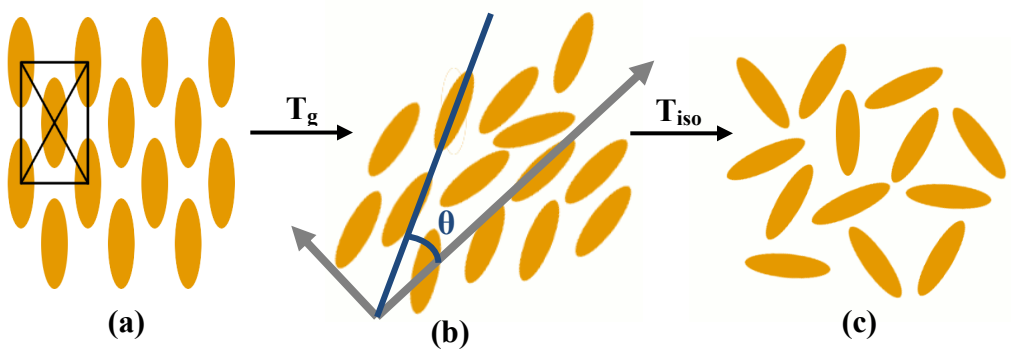

Figure 1. Mesogen alignment in the (a) crystalline, (b) liquid crystalline (assembly director is shown in gray and angle of alignment with respect to the assembly director in LC phase is shown in blue), and (c) isotropic phase.

The isotropic phase can be accessed either above or below the melting temperature (T_m) of the polymer, thus the temperature at which the isotropic phase is first

present will be referred to simply as the isotropization temperature (T_{iso}). The range of temperature over which the mesophase exists will be referred as ΔT_{LC}.

Figure 2. Diagram showing the 2-D order of the smectic mesophase and 1-D order of the nematic mesophase.

Mesophases are classified based on their ordering characteristics. The most common mesophases found in thermotropic LCPs are nematic and smectic, seen in Figure 2, which consist of 1-dimensional order and 2-dimensional order, respectively; the 2-D smectic mesophase is considered more ordered than the 1-D nematic mesophase[8]. The degree of ordering is determined by the order parameter, *S*, which is given as the following average:

$$S = \frac{3\langle \cos^2 \theta \rangle - 1}{2}$$

where θ is the angle between the individual molecule axis and the assembly director as seen in Figure 1b. *S* for liquid crystals will range from 1, indicating complete parallel alignment with respect to director, to -½, indicating complete perpendicular alignment with respect to the director. An *S* value of 0 indicates complete disorder (isotropic).

It is due to the ordering of the mesogens that the polymer chains order and pack efficiently, giving LCPs inherently low gas permeabilities. Although the low permeability (P; P = D x S) in these polymers is mainly attributed to low solubilities (S), their diffusivities (D) are also significantly lower than the most commonly used barrier polymer polyethylene terephthalate (PET) as seen in Table 1[2]. This has made LCPs attractive candidates for packaging applications leading to barrier studies of LCPs in bulk

and multilayer films[9,10]. However, these studies have focused on films with thicknesses ranging from 2.5 to 150 μm with a maximum of three layers. Other barrier applications for which LCPs have been considered include protective coatings for microelectronics, electrical cables, flexible displays and solar panels[10].

Table 1. Comparison of LCP P, D and S to PET[2]. For this table, $P = \frac{D \times S}{76}$ to account for unit conversions.

Gas	Polymer	Permeability (P) X10^2 (Barrer)	Diffusivity (D) X 10^{10} (cm^2/sec)	Solubility (S) X 10^2 (cm^3 (STP)/cm^3 atm)
O_2	PET[a]	11	95	9
	HIQ-40 (annealed)[b]	1	12	6
	LCP[c]	0.05	8	0.05
N_2	PET[a]	1.7	32	4
	HIQ-40 (annealed)[b]	0.14	6	1.8
	LCP[c]	0.004	1.5	0.2
CO_2	PET[a]	43	16	200
	HIQ-40 (annealed)[b]	3	5	40
	LCP[c]	0.08	1	7

[a] amorphous poly(ethylene terephthalate); reduced by a factor of 2 when semicrystalline
[b] HIQ-40 = 40/30/30 *p*-hydroxybenzoic acid/isophthalic acid/hydroquinone
[c] LCP = 73/27 *p*-hydroxybenzoic acid/6-hydroxy-2-naphthoic acid (HBA/HNA)

As stated before, LCP material properties are closely linked to both the LC content and the ordering. Studies have showed an increased barrier (i.e., a decreased permeance) as a function of phase ordering, with the contribution to the decreased permeability coming from decreases in both solubility and diffusivity, as stated before. For instance, a study of a cross-linked polysiloxane LC elastomer for drug delivery showed the solubility is a function of the LC content[11]. Likewise, the LC elastomer also showed that an increase in LC content leads to a decrease in the diffusivity. However, since the low gas permeabilities have been mostly attributed to low solubility, research has focused on understanding the gas solubility process.

MATERIALS

During the course of this research we worked with main chain, side chain, and hydrogen bonded liquid crystalline polymers. Below is a detailed explanation of each material type.

Main Chain Liquid Crystalline Polymers

All commercially-available LCPs from suppliers such as Ticona, Solvay and Polyplastics are main chain liquid crystalline polymers. Main chain liquid crystalline polymers (MCLCPs) have the mesogen incorporated into the polymer backbone as shown in Figure 3a, where the yellow oval represents the mesogen.

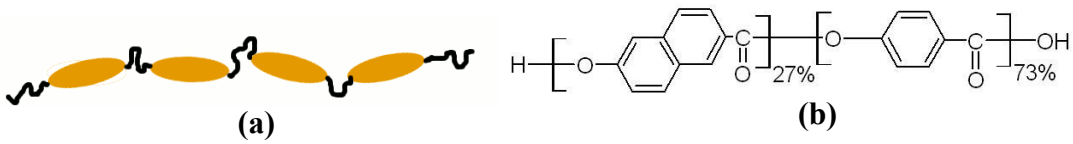

(a) **(b)**

Figure 3. Structure of (a) main chain liquid crystalline polymer and of (b) Vectra A950.

The MCLCPs used in this study were from the commercially-available Vectra series by Ticona. Figure 3b shows the structure of one of the grades of Vectra that was studied. These MCLCPs have viscosities which are very low and strongly dependent on temperature, making film layering by melt-state processes very challenging. Typical polymers used in film extrusion are processed at temperatures 200-300 °C and exhibit viscosities in the range of 100-100000 Pa·s at high shear rates (close to 100 rad/s or 100 s^{-1}). Figure 4 shows the viscosity of Vectra A950 as a function of steady shear rate at 290 °C. Looking at these data, the viscosity for Vectra A950 under these conditions (high temperature and high shear rate) would be lower than 100 Pa·s. For this reason, the viscosity of these MCLCPs has to be increased before they can be multilayered into thin film layers and studied under confinement.

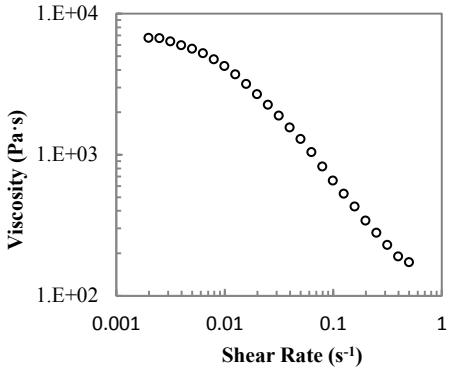

Figure 4. Dependence of viscosity on steady shear rate for Vectra A950 at 290 °C under 2% strain.

Hydrogen Bonded Liquid Crystalline Polymers

Hydrogen bonded liquid crystalline polymers are of interest because of their easy synthesis, which usually consists of mixing the components either in solution or in the melt-state. This type of LCP has been extensively studied[12-14] with the first supramolecular LCPs consisting of MCLCPs formed by hydrogen bonding small

molecules, LC or non-LC, in solution. For this research, a hydrogen bonded side chain liquid crystalline polymer (HBLCP) was synthesized by mixing a commercially available polymer containing hydroxyl functional groups (polyhydroxystyrene or copolymers of ethylene and acrylics) with a small molecule mesogen in the melt state to create a side chain liquid crystalline polymer as shown in Figure 5. This allows the use of commercial polymers as backbones or parent polymers. It also facilitates the industrial implementation and scale up of the synthesis.

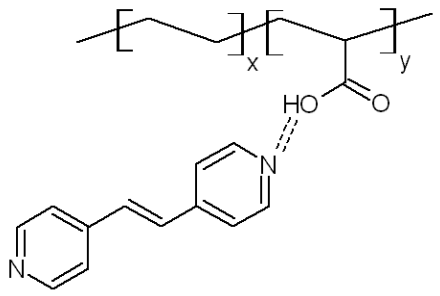

Figure 5. Structure of hydrogen bonded side chain liquid crystalline polymers (HBLCPs) used in this research.

Side Chain Liquid Crystalline Polymers

Side chain liquid crystalline polymers (SCLCPs) have their mesogens covalently attached to the polymer backbone through a flexible spacer, commonly an alkyl chain, as shown in Figure 6. The complete synthesis of the SCLCP, as shown in Figure 7-9, allows easy modifications such as flexible spacer length and mesogen chemistry, which directly affects the properties of the SCLCP.

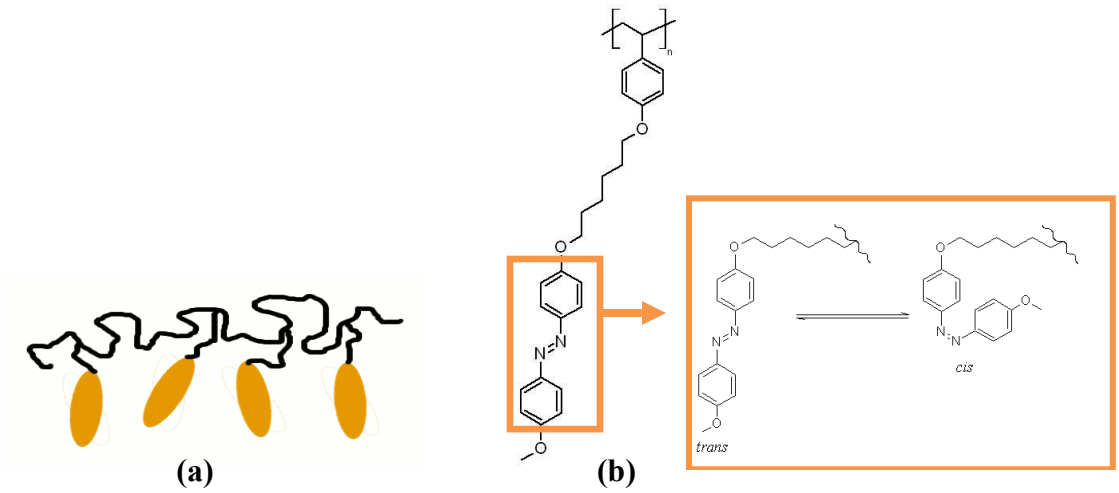

Figure 6. Structure of (a) side chain liquid crystalline polymers and (b) the side chain liquid crystalline polymer synthesized for these studies. Highlighted is the azobenzene molecule and its trans and cis isomers.

The azobenzene-containing SCLCP used, shown in Figure 6b, was synthesized using the wet chemistry methods described in the next section and can exhibit both nematic and smectic mesophases [15]. The LC azobenzene molecule, highlighted in Figure 6b, has the unique ability to photoisomerize from the stable *trans* to the less stable *cis* conformation when it's exposed to a certain wavelength of light. While the mesogens are able to pack efficiently when in the compact *trans* conformation, the bulkiness of the *cis* conformation will cause the LC phase ordering to be lost regardless of the temperature [16]. This allows the possible manipulation of the LC phase at any temperature above T_g. Other advantages of this material are that this SCLCP is soluble in common organic solvents unlike commercially-available MCLCPs, and the synthesis can be easily scaled up.

It was first assumed that the viscosity of the SCLCP homopolymer shown in Figure 6b would be too low for melt processing into multilayers, just like commercial

MCLCPs. Therefore, a triblock copolymer was examined first because PS end blocks can provide melt strength and enhance the viscosity of the final SCLCP.

EXPERIMENTAL METHODS

An assortment of methods had to be used to obtain liquid crystalline polymer films to be studied. Both wet chemistry and melt-state chemistry were employed to synthesize suitable LCPs. Methods used for the manufacturing of multilayered films are also covered in this section.

Wet Chemistry Methods

Anionic Polymerization

Anionic polymerization was used to synthesize triblocks of polystyrene-polyhydroxystyrene-polystyrene (PS-PHOS-PS) as the polymer backbone for the SCLCPs in this research. In this reaction mechanism, shown in Figure 7, potassium naphthalenide initiator was used in conjunction with α-methylstyrene to form a dicarbanion[17], which is able to propagate in two directions. *Tert*-butoxystyrene monomer was added followed by the addition of styrene to form the triblock, where the amount of styrene and *tert*-butoxystyrene monomer added depends on the desired composition of the final triblock. The anionic polymerization was finally terminated by the addition of excess methanol to form a polystyrene-poly(*tert*-butoxystyrene)-polystyrene (PS-PtBOS-PS) triblock. Once the triblock is precipitated, gravity filtered and dried under vacuum overnight, the poly(*tert*-butoxystyrene) block can undergo acid hydrolysis to remove the *tert*-butoxy group and replace it with a hydroxyl group. A 10% weight by volume solution of the triblock PS-PtBOS-PS in acetone was refluxed with five times molar excess hydrochloric acid (HCl) for 5 hours to obtain the PS-PHOS-PS triblock[18].

Successful hydrolysis as well as the composition of the block copolymer was verified by proton nuclear magnetic resonance (^{1}H-NMR).

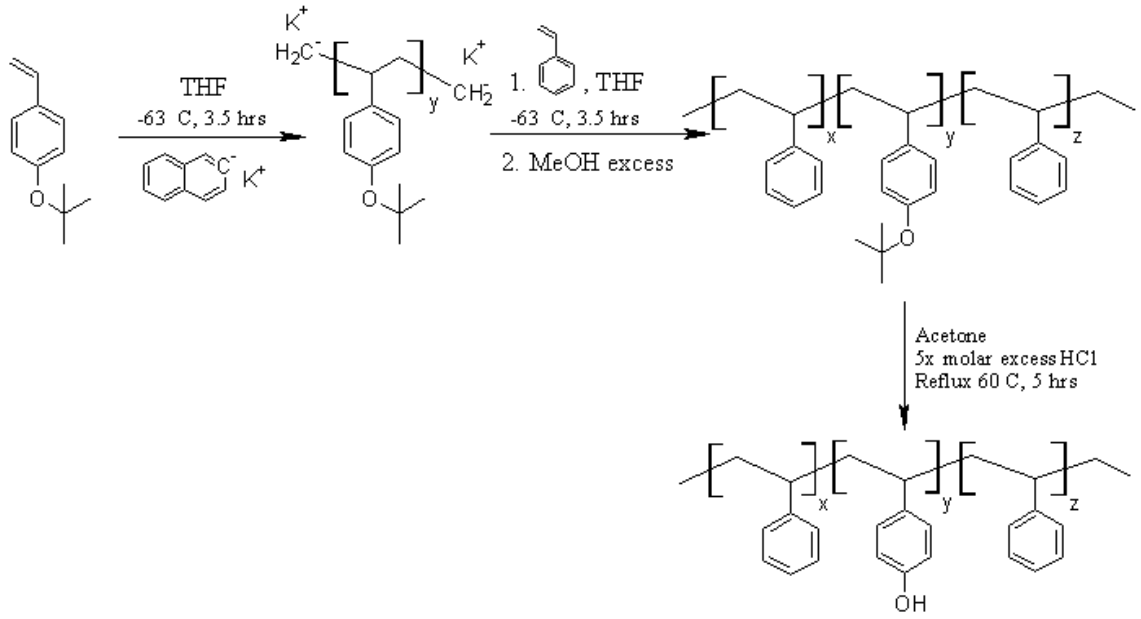

Figure 7. Reaction scheme of anionic polymerization followed by acid hydrolysis for the synthesis of PS-PHOS-PS triblock.

Diazotization followed by Coupling

In order to synthesize the LC mesogen of interest, a diazonium salt had to be first synthesized followed by coupling as seen in the reaction scheme in Figure 8.

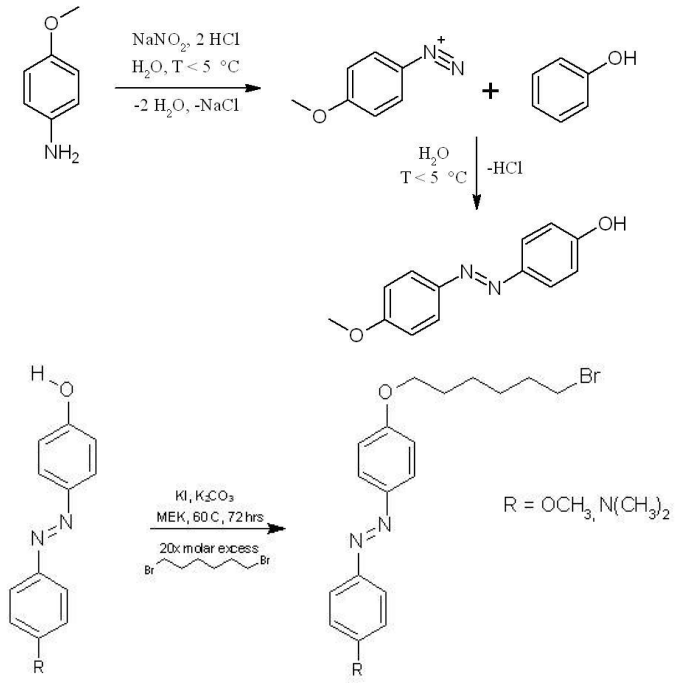

Figure 8. Reaction scheme for the synthesis of the desired azobenzene-containing LC mesogen.

Following literature[15], 0.41 moles of p-anisidine was dissolved in a 3M hydrochloric acid (HCl) solution and chilled to a temperature lower than 5 °C. Sodium nitrite in a 2.8 M aqueous solution was then added slowly to the acid solution while maintaining the low temperature. Lastly, a 1M aqueous solution of phenol and sodium hydroxide (NaOH) in the ratio of 0.41 to 1, respectively, was added to the mixture slowly while vigorously stirring and maintaining the temperature below 5 °C. The final solution was then brought to room temperature, stirred for an additional hour, gravity filtered, and washed with deionized water until a neutral pH was achieved. Once the diazonium salt was synthesized, it was dried overnight under vacuum. The diazonium salt (13.4 mmol) was then dissolved in methyl ethyl ketone (MEK) with 20 times molar excess of 1,6-dibromohexane, potassium iodide (0.15 mmol KI) and potassium carbonate (21.44 mmol

K_2CO_3) and refluxed for 72 hours under a dynamic argon atmosphere. The final mixture was then cooled to room temperature and gravity filtered to remove the excess K_2CO_3 and KBr formed. To remove the MEK from the mixture, the filtrate was then dried on a rotovap. The final orange, viscous solution was diluted in hexane and cooled to induce crystallization[15,19]. The final yellow LC mesogen crystals were filtered and dried under vacuum before attaching to the polymer backbone. Successful synthesis as well as removal of all impurities was verified by ^{1}H-NMR before proceeding.

Two different azobenzene mesogens, a tertiary amine end group (NMe) with a hexamethylene flexible spacer and a methoxy end group (OMe) with a hexamethylene flexible spacer, were prepared. The difference between these, other than their polarity, is that the NMe version absorbs and photoisomerizes in both ultraviolet and violet light while the OMe version absorbs and photoisomerizes only when exposed to UV light.

Williamson Etherification

Starting with polyhydroxystyrene (PHOS) either in a triblock (PS-PHOS-PS) or commercial PHOS (Polysciences Inc, MW=22,000 g/mol), the LC mesogen was attached using Williamson etherification as delineated in literature[15,19]. A mixture of 2.5 mmol PHOS, 2.75 mmol LC mesogen, 0.25 mmol *tetra*-n-butyl ammonium and 3.5 mmol NaOH was dissolved in a 1:1 volume ratio of MEK and toluene to make a 0.141 M solution. This solution was then refluxed for 48 hours, cooled to room temperature and diluted in dichloromethane (DCM). Subsequent liquid-liquid extractions were performed of the DCM layer with deionized water until the pH and the conductivity of the water was restored. The DCM layer was then dried with sodium sulfate ($NaSO_4$), filtered, and dried on a rotovap to remove excess DCM. Once completely dried, the light orange powder was dissolved in a small amount of DCM and precipitated in methanol (MeOH). If all the

water was not completely removed from the DCM solution before it is dried on a rotovap, the final polymer will not dissolve in DCM to be precipitated in MeOH. The precipitate polymer was then filtered and dried under vacuum. To remove the unreacted LC mesogen, the polymer was Soxhlet extracted in MeOH for 2 days and dried under vacuum. The final product is a SCLCP where the mesogens hang off the backbone of the polymer as seen in Figure 9.

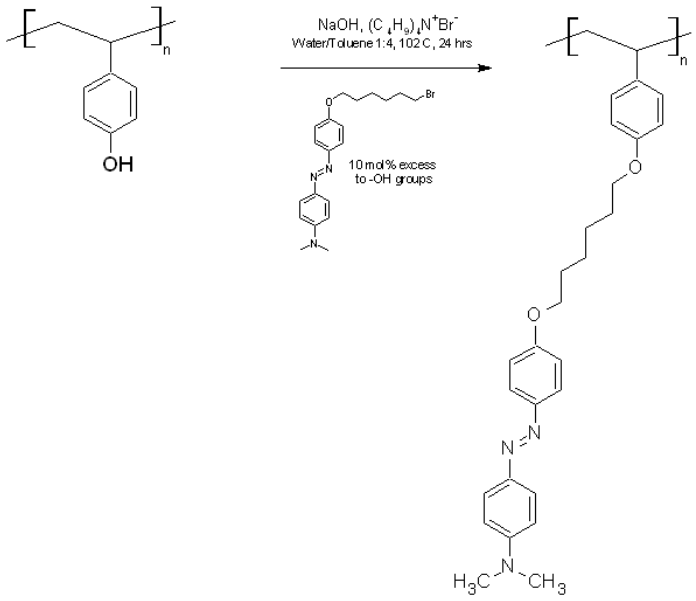

Figure 9. Reaction scheme for the functionalization of PHOS to synthesize the SCLCP.

The mesogens mentioned in the previous section (NMe and OMe) were used to prepare homopolymers (LCP_{OMe}, LCP_{NMe}) and triblocks with both 46 mol% and 36 mol% LCP (PS-46LCP_{OMe}-PS, PS-46LCP_{NMe}-PS, and PS-36LCP_{NMe}-PS).

Melt-State Chemistry Methods

Melt Compounding

Melt compounding was performed in a DSM Xplore microcompounder. The polymer was added as pellets to the hopper with the chosen amount of additive and allowed to mix and react for the desired amount of time under dynamic dry nitrogen atmosphere. The resulting polymer was then extruded out of the DSM microcompounder and cut into pellets for further processing or analysis.

Commercially-available MCLCP Vectra A950 (73 mol% *p*-hydroxybenzoic acid, 27 mol% 2,6-hydroxynaphthoic acid) was compounded in the melt-state with different amounts of triphenyl phosphite (TPP) in an attempt to exploit reported chain extension reactions accomplished with other polyesters such as PET and poly(butylene terephthalate) (PBT)[20-27]. Compounding time was varied in order to find optimum reaction conditions. Samples were made with 1 to 5 wt % TPP and processed from 5 to 30 minutes at 290 °C and 100 rpm. However, during melt-compounding TPP vapors emanated from the chamber due to its lower boiling point. For this reason, the final amount of TPP in each reacted batch is not the same as the initial amount of TPP added to the hopper as is later shown in the results section. The different samples obtained will be referred to by the initial amount of TPP added. All the final samples were dried under high vacuum at high temperatures to remove all unreacted TPP and by-products.

To obtain the HBLCPs in this study the mesogen 1,2-Di(4-pyridyl)ethylene (DPE) was melt-mixed with several copolymers based on poly(ethylene)-co-poly(acrylic acid) (PE-co-PAA; Aldrich Cat. No. 18,104-8), poly(ethylene)-co-poly(methacrylic acid) (PE-co-PMAA; DuPont Nucrel 925), or PHOS (MW: 22000 g/mol; Polysciences, Inc) in order to find a system with suitable viscosity and thermal stability that would enable further melt-processing into film. An ionomer based on the poly(ethylene)-co-

poly(methacrylic acid) (PE-co-PMAA) copolymer with 29% Na+ neutralized MAA (DuPont Surlyn 8940) was also used since ionomers are known to have higher melt strength and viscosity than their non-ionized equivalents[28]. These liquid crystalline ionomers (LCIs), which result from the interaction of mesogens with ionomers, have also been greatly studied as non-covalent alternatives for LCPs[29]. During the synthesis of HBLCPs, the LC content can be controlled either through the amount of LC added to the compounder or by the volume fraction of functional groups available for hydrogen bonding on the parent polymer. HBLCPs synthesized for this project contained 1:0.5 or a 1:1 ratio of non-neutralized hydroxyl functional groups in the polymer to amine functional groups in DPE (i.e., 0.25 DPE molecules or 0.5 DPE molecules per 1 carboxyl functional group in the polymer, respectively).

Other Methods

Film Fabrication

SCLCP multilayer thin films were made with layers of LCP_{OMe} confined on both sides by a non-LC polymer (i.e., no air or substrate interface) as shown in Figure 10. Polymers used as confining layers must have a T_g above T_{iso} of the LCP_{OMe} to ensure the integrity of the layers at all annealing temperatures of interest. Finding the appropriate complimentary polymer for multilayering with the LCP_{OMe} was the biggest challenge in film preparation since both polymer and solvent from which it was cast could not interfere with the SCLCP. After trying polycarbonate (PC; DuPont), polyimide P84 (Evonik), and poly(ethylene-co-norbornene) (PEN; Polysciences) in a wide range of casting solvents, it was determined that PEN was the best option. Solubility tests of both PEN and LCP_{OMe} were conducted in several solvents to find a solvent system for multilayered thin film preparation. A solution of 2 wt % PEN in cycloheptane was

prepared and spin coated into multilayered films as the confining layer. On the other hand, solutions of varying concentrations were made of the LCP_{OMe} in cyclohexanone in order to manipulate the layer thickness. After each layer was spin coated, the substrate was soft-baked at a temperature above the boiling point of the casting solvent to completely dry the polymer layer. The layer thickness was then measured using a J. A. Woolam M-2000 ellipsometer to verify that the polymer layer was completely dry before spin coating the next layer (i.e., the film was completely dry if the layer thickness did not change with additional annealing). Layer thicknesses for the LCP_{OMe} were 800 nm (total 3 layers), 300 nm (total 5 layers), 100 nm (total 17 layers), and 50 nm (total 13 layers), while the confining polymer layer thickness was always approximately 200 nm. The total LCP content in the multilayered thin films was kept constant regardless of LCP layer thickness, i.e., if the individual layer thickness decreased, the number of layers increased, with the exception of films with 50 nm LCP_{OMe} layers. It was found that a LCP_{OMe} layer thickness below 50 nm would be dissolved once the next layer was casted, even after soft-baking, while thicknesses of 50 nm could not be stacked higher than 13 total layers without cracking in the layers. Multilayered films were spin coated onto silicon, glass or quartz substrates.

Figure 10. Multilayered films with multiple LCP layers prepared for characterization, where the blue represents the confining polymer layer and the orange represents the LCP layer.

The film arrangement in Figure 10 allowed the study of confinement effects on the LCP without the effect of air interfaces. Although SCLCPs have been studied in thin films, none of these studies have addressed multilayer films or films where the LCP is confined on both sides by a polymer, with the exception of LCPs within block copolymer microdomains. Commercial LCPs, i.e. MCLCPs, have been previously multilayered with non-LCP layers, but the films were composed of at most 3 layers with LCP layer thicknesses of 2.5 μm or greater[10].

Results and Discussion

Main Chain Liquid Crystalline Polymers

Successful modification of Vectra with TPP was confirmed through the study of the viscosity of the MCLCP, Fourier Transform Infrared (FT-IR) spectroscopy, combustion analysis, wide angle X-ray diffraction (WAXD), and polarized optical microscopy (POM). An increase in the viscosity of the melt indicates that chains have increased in molecular weight, combustion analysis and FT-IR peaks can detect the presence of phosphorus bonds in the samples, while WAXD and POM can confirm the retention of LCP character of Vectra.

The viscosity of Vectra-TPP samples are presented in Figure 11. The greatest viscosity improvement was observed when 4 wt % TPP was added and mixed for 30 minutes. The viscosity in this case increased to 20 times that of neat Vectra. As TPP was added up to 4 wt%, the viscosity increased progressively until 5 wt% TPP was added. It is hypothesized that the addition of 5 wt% TPP changes the reaction mechanism to favor the chain termination shown in the bottom-most reaction in Figure 12, as well as a shift of reaction equilibrium towards the reagents due to the excess of phenol by-product (Le Chatelier's principle).

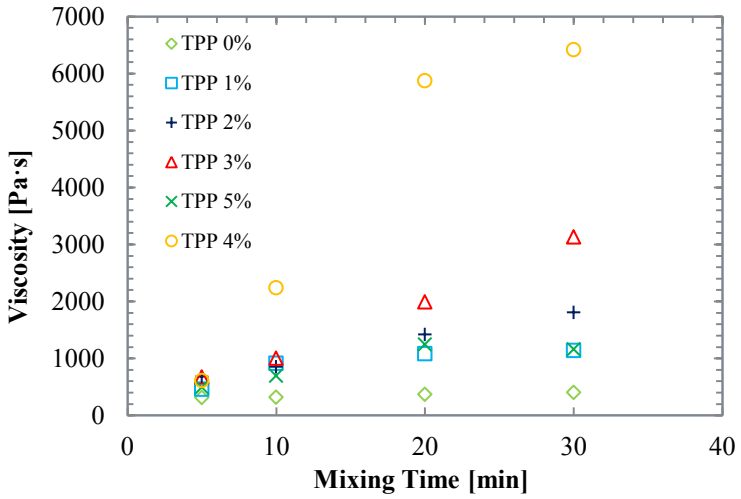

Figure 11. Steady shear viscosity at 0.16 s^{-1} shear rate for Vectra samples compounded with 0 (◊), 1 (□), 2 (+), 3 (Δ), 4 (O), and 5 (x) wt % TPP at 290 ^{o}C as a function of mixing time[30].

The presence of phosphorus in the Vectra-TPP samples was confirmed by combustion analysis, which indicates there were 990, 260 and 0 ppm elemental phosphorus in samples with 4 wt%, 2 wt% and 0 wt% TPP, respectively. There was also an increase in the phosphorus-oxygen bond peak in the FT-IR spectra, supporting the synthetic route presented in Figure 12. Yet, when the Vectra-TPP samples were reprocessed in air, in a similar manner to how they would be processed into film, a decrease in viscosity was observed that almost reached the viscosity of neat Vectra presumably due to the scission of the P-O bonds[30]. Other candidate viscosity modifying additives are currently under investigation by other group members. Nonetheless, this study demonstrated proof of principle for these subsequent studies.

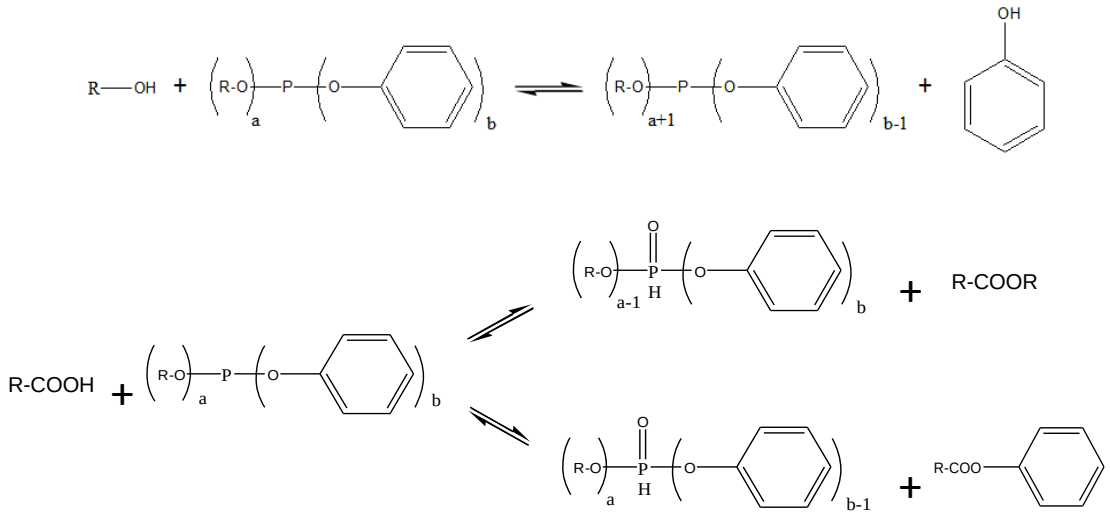

Figure 12. Reaction mechanisms between TPP and hydroxyl or carboxyl end groups, where R represents the Vectra polymer chain, and a + b = 3[25-27].

When studied under POM, Vectra still exhibited LC properties after reaction with TPP as seen in Figure 13a. WAXD spectra of Vectra (Figure 13b) before and after TPP addition showed no change in the crystal structure. The glass transition, melting and crystallization temperatures of Vectra also remained unchanged after reaction with TPP, regardless of the amount of TPP added. These studies imply the intrinsic structure of Vectra was unaffected by the viscosity modification procedure.

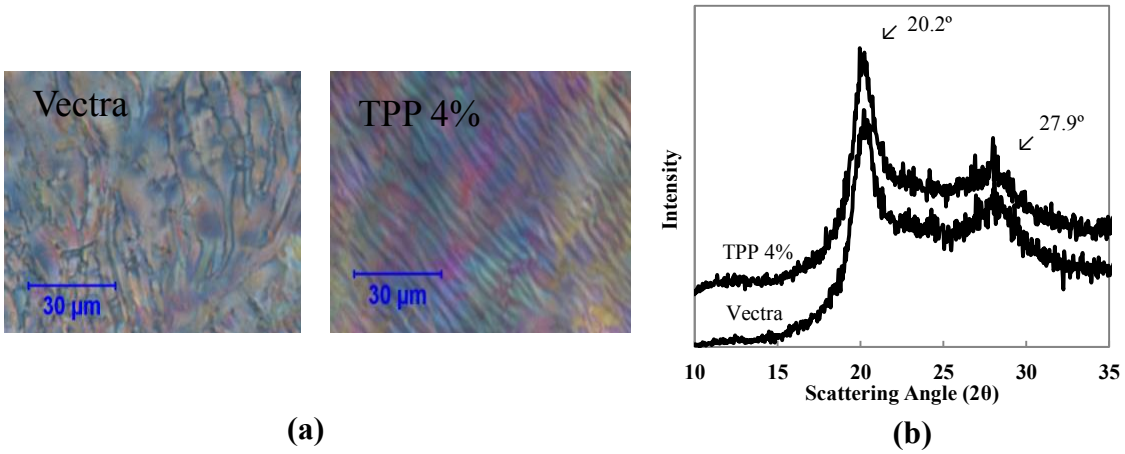

Figure 13. (a) Polarized optical microscopy images and (b) WAXD spectra of Vectra before and after TPP addition[30].

HYDROGEN BONDED LIQUID CRYSTALLINE POLYMERS

After the formation of the HBLCPs by melt mixing a mesogen that hydrogen bonds with the polymer, rheology measurements were conducted to determine if these materials were good candidates for melt processing into films. PHOS based HBLCPs were found to decompose before melting, similar to the PHOS precursor. PE-co-PMAA and PE-co-PAA based HBLCPs had suitable viscosities for multilayering coextrusion (ranging from 100-10000 Pa·s) when compared to commercial PS. Nonetheless these values of viscosity were obtained at temperatures too low (80-90 °C) since most require processing temperatures above 200 °C.

PE-co-PMAA ionomer (DuPont Surlyn 8940) based LCIs exhibited suitable viscosities for melt processing at a temperature of 185 °C as shown in Figure 14, where PS is added as a viscosity reference for comparison (i.e., typical film extrusion viscosity at a typical PS extrusion temperature). The higher melting temperature of LCIs allows for a wider range of commercial polymer choices for multilayer coextrusion.

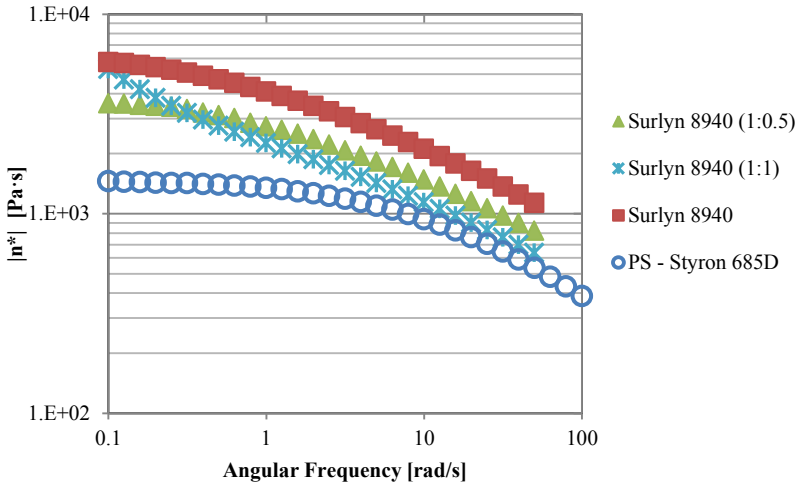

Figure 14. Steady state viscosity of LCIs with different amounts of DPE mesogen added. PS is added as a reference for comparison. Viscosity of LCIs was measured at 185 °C, while the viscosity of PS was measured at 240 °C.

However, when studied by thermogravimetric analysis (TGA) the LCIs showed a significant decrease in weight starting around 167 °C when run in air atmosphere (Figure 15). After further consideration it was determined that the LC mesogen chosen (DPE) degrades at that temperature causing a drop in the sample weight[13]. It's also seen that the greater the amount of DPE added, the greater the drop in the weight percent of the sample. Thus, these LCIs would have to be melt processed at a temperature of 160 °C or lower, which is well below typical film extrusion temperatures of 200-300 °C.

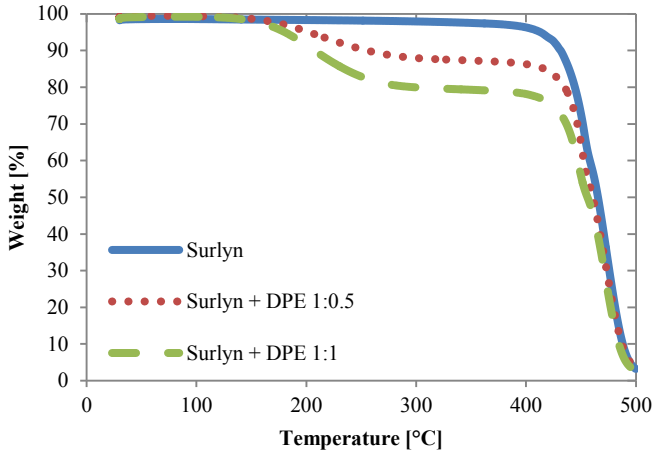

Figure 15. Thermogravimetric analysis (TGA) results of PE-co-PMAA ionomer (15 wt% MAA, 29% neutralized Na^+) before and after the addition of LC mesogen 1,2-Di(4-pyridyl)ethylene (DPE). TGA was run under air atmosphere. Significant weight loss starts around 167 °C due to the degradation of DPE.

Of all systems studied, the LCI (PE-co-PMAA ionomer with DPE) had the best thermal and rheological properties, and exhibited small isolated LC domains throughout the sample when observed under POM as shown in Figure 16a. This was true even when the DPE was present in a 1:0.5 ratio of un-neutralized carboxyl functional groups in the Surlyn ionomer to amine functional groups in DPE (i.e., 0.25 DPE molecules to 1 carboxyl functional group of the polymer). However, experiments to confirm that the LC domains were confined within the ionomer clusters as described in literature[8,29], were inconclusive. WAXD studies presented in Figure 16b show no significant changes after the addition of LC mesogens more than likely because ionomer clusters, which overlap with peaks for the PE crystals, are more prevalent than the LC domains and dominate the scattering.

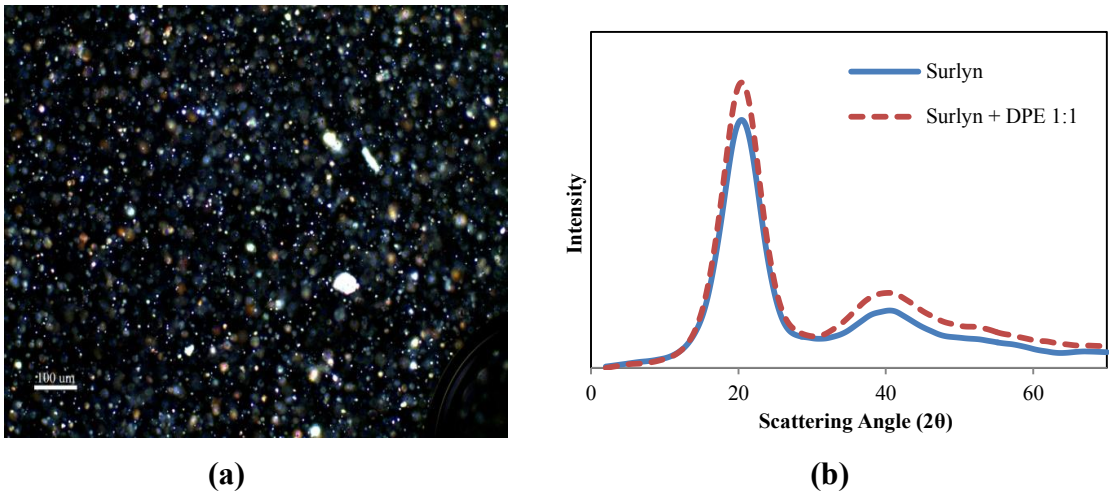

(a) **(b)**

Figure 16. (a) Polarizable optical microscopy of Surlyn 8940 (PE-co-PMAA, 15 wt% MAA, 29% neutralized Na^+) with 1,2-Di(4-pyridyl)ethylene (DPE) mesogen in a 1:0.5 ratio, respectively, taken at 150 °C. (b) WAXD spectra of Surlyn 8940 ionomer before and after the addition of mesogen DPE.

SIDE CHAIN LIQUID CRYSTALLINE POLYMERS

Synthesis and Polymer Characterization

Since the Williamson etherification was conducted in the laboratory under ambient conditions, it is hypothesized that the mesogen absorbed visible light and photoisomerized into the *cis* conformation making it hard to attach to the PHOS backbone due to steric hindrance. Complete functionalization of the PHOS was only achieved once the reaction was run under filtered light. Successful synthesis of these polymers was verified by proton nuclear magnetic resonance (^{1}H-NMR) and gel permeation chromatography (GPC) as shown in Figure 17 and 18. As expected the GPC traces in Figure 17 show a shift first to higher elution volumes (lower hydrodynamic volume) after acid hydrolysis of PtBOS due to a decreased molecular weight, and then a shift to lower elution volumes due to the functionalization of the PHOS block and an increase in molecular weight.

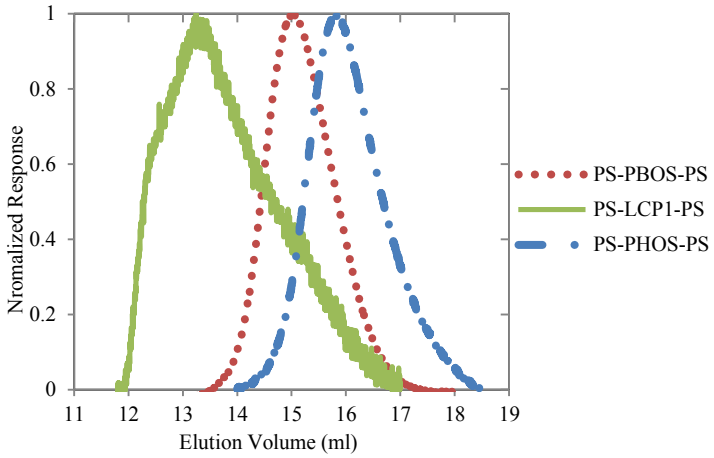

Figure 17. GPC traces of SCLCP triblock PS-LCP_{NMe}-PS showing successful synthesis.

^{1}H-NMR spectra in Figure 18 show the disappearance of the –OH peak at 7.8 ppm when LC functionalization of PHOS occurs, as well as the appearance of sharp peaks at 3.8 ppm and 3 ppm corresponding to the –O-CH_2 bonds created and the amine on the LC, respectively. The amount of functionalization achieved can be calculated using the area under these characteristic peaks. All SCLCPs synthesized for this project were deemed successful if functionalization of the hydroxyl groups was 98 ± 2%. During the final synthesis step of these polymers (Williamson etherification) a direct correlation between reagent concentration and percent functionalization was observed, which could allow the systematic control of percent functionalization of PHOS.

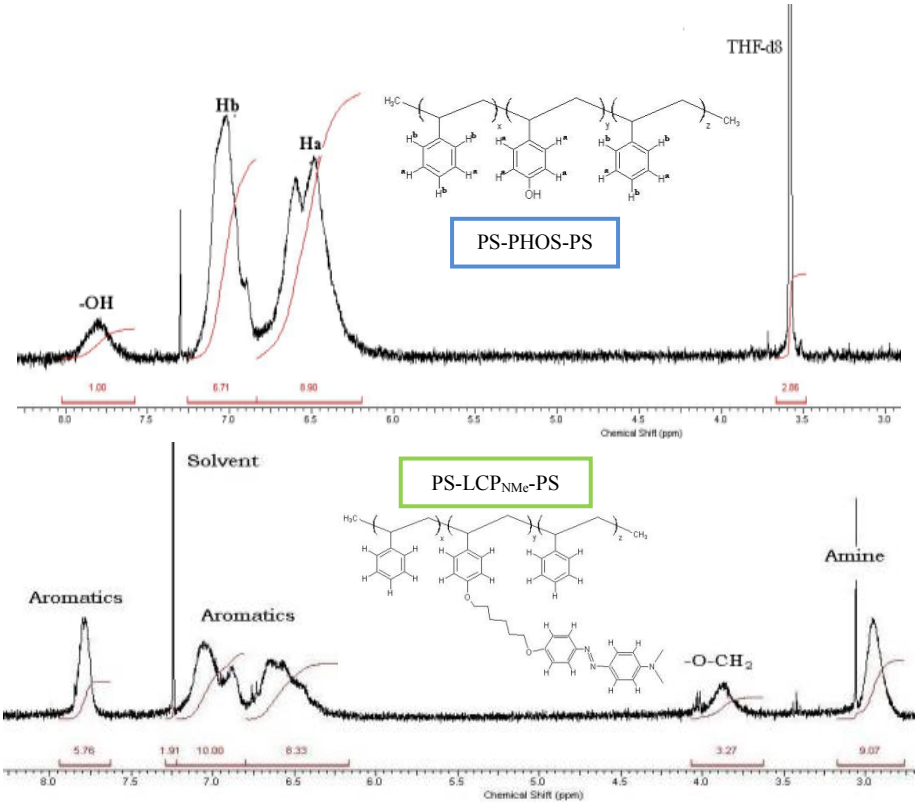

Figure 18. ^{1}H-NMR spectra of PS-PHOS-PS (in THF-d_8) and PS-36LCP$_{NMe}$-PS (in $CDCl_3$) after functionalization and removal of unreacted LC mesogen. Percent functionalization can be calculated from the area under the peaks corresponding to –O-CH_2, amine, and –OH.

Due to the complexity of block copolymer microphase separation and the inability of triblocks that were 100% functionalized to flow when heated (i.e., they only behaved as a paste when heated before degrading and can't be melt-processed), these materials (PS-46LCP$_{OMe}$-PS, PS-46LCP$_{NMe}$-PS and PS-36LCP$_{NMe}$-PS) were not further considered. The rest of the study focused on SCLCP homopolymers, specifically LCP$_{OMe}$, since it can easily be synthesized under laboratory ambient conditions. Still, the change from a triblock to commercial PHOS backbone brought with it some solubility and synthesis challenges that were only overcome after the solvent for the Williamson etherification was changed to a 1:1 mixture of methyl ethyl ketone (MEK) and toluene. Unfortunately,

GPC results for LCP_{OMe} or LCP_{NMe} could not be obtained due to column interaction, and successful synthesis had to be confirmed only through ^{1}H-NMR. The molecular weight of LCP_{OMe} could only be calculated theoretically as 76,000 g/mol based on the reported PHOS molecular weight and the molecular weight of the mesogens added.

Differential scanning calorimetry (DSC) of LCP_{OMe} in Figure 19 showed two distinct transitions at 96 °C (T_g) and 146 °C (T_{iso}) upon heating indicating the presence of one mesophase (ΔT_{LC} of 50 °C), which coincided with data presented in literature[31,32]. When LCP_{OMe} is heated above T_g the polymer transitions from a yellow powder to an orange paste that could be manipulated and molded. Once LCP_{OMe} is heated above T_{iso}, the polymer turns a vibrant clear orange color and flows much like a viscous liquid.

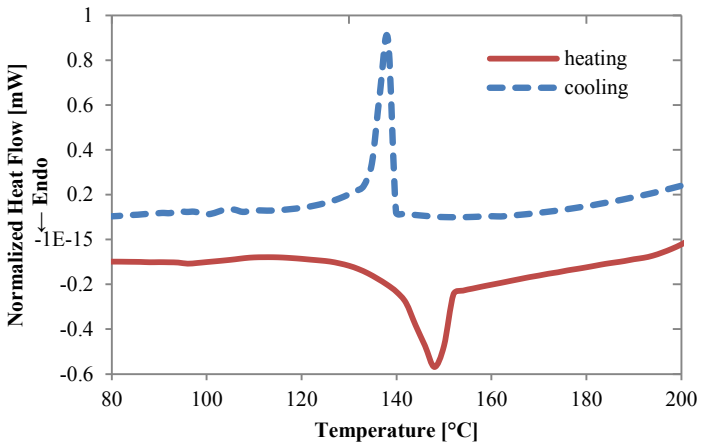

Figure 19. DSC thermogram of LCP_{OMe}.

POM images taken as a function of temperature support the presence of one mesophase, yet the LC domains were too small to define the type of mesophase. Imrie and coworkers have reported this same difficulty in developing textures for mesophase identification with the aid of POM[32]. WAXD spectra of the bulk LCP_{OMe} showed no

distinct LC peaks even after being annealed for 3 days above T_g, further complicating the assignment of a mesophase.

Photoisomerization wavelengths were obtained by conducting UV-Vis spectroscopy studies of dilute solutions of the mesogen and SCLCP homopolymers. Figure 20 shows the maximum absorption of the NMe mesogen in the violet visible light range while the maximum absorption of both the OMe mesogen and LCP_{OMe} homopolymers is in the UV light range. This maximum absorption corresponds to the wavelength responsible for the photoisomerization into the *trans* conformation of the azobenzene unit. The wavelength responsible for the photoisomerization into the *cis* conformation of the azobenzene unit can be seen as the smaller peak in the 450 nm region for the OMe mesogen and LCP_{OMe} homopolymer. The wavelength responsible for the photoisomerization into the *cis* conformation of the NMe mesogen is not seen in Figure 20.

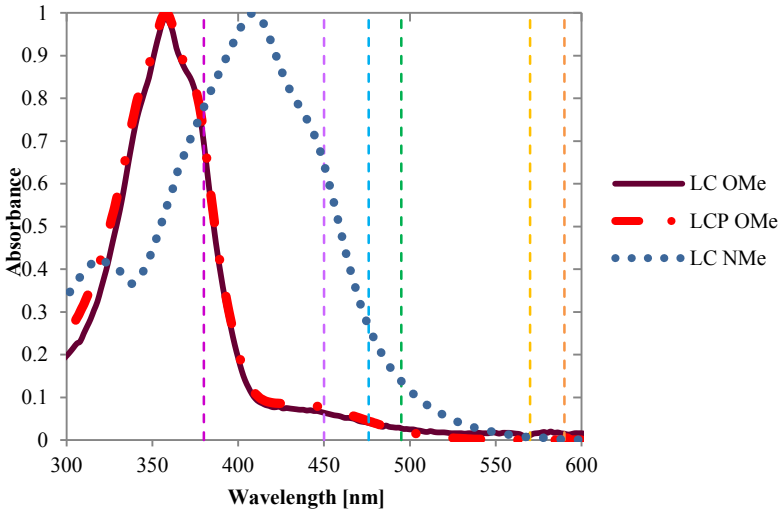

Figure 20. UV-Vis absorption spectra of mesogens LC_{NMe}, LC_{OMe}, and homopolymer LCP_{OMe}.

Lastly, the viscosity of the LCP_{OMe} homopolymer was measured using a rheometer and a cone and plate geometry to check the possibility of melt processing this polymer. Unfortunately, the viscosity of the LCP_{OMe} in the melt at 160 °C (above T_{iso}) was in the 10-30 Pa·s range (compared to the typically required viscosity of 100-10000 Pa·s at temperatures of 200-300 °C for film extrusion), making it an unfit material for multilayered coextrusion.

Confinement Studies

Following the objectives of this project, the best performing material of those studied, in this case the side chain liquid crystalline polymer LCP_{OMe}, was layered with a complementary polymer into thin films to study the confinement of the LCP. This section details the characterization of the films as-cast as well as after thermal annealing and photoaligning the LCP layers.

As-cast Characterization

Multilayered films were characterized as-cast to serve as a control for the confinement studies. The layer integrity of the films was studied under a scanning electron microscope (SEM). Multilayered films on a silicon substrate were flash frozen in liquid nitrogen and subsequently fractured in order to prepare them for the SEM. Figure 21 shows the cross-section of the films under SEM. Because thinner SCLCP layers lack rigidity, the layers on the films with 100 nm and 50 nm layers (Figure 21 b and c) could not be uniformly cut after freezing. Better images of the cross-section of the films could be obtained if the films were microtomed rather than freeze-fractured before observing them under the SEM.

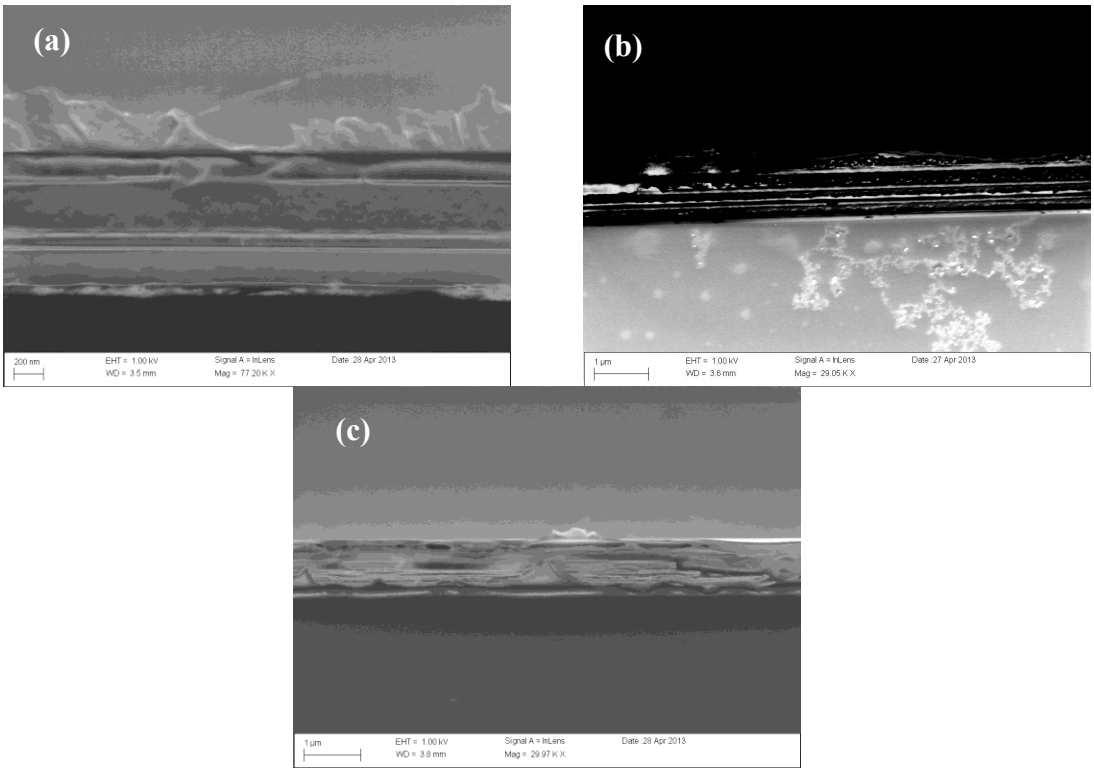

Figure 21. Scanning electron microscopy (SEM) images of freeze fractured multilayered films with SCLCP layer thicknesses of (a) 300 nm, (b) 100 nm, and (c) 50 nm.

When studied under POM to verify the preservation of the LC behavior of films, no pattern was visible under cross polarizers when the LCP_{OMe} layers were confined by PEN on both sides. It is possible that no pattern is observed because the LC mesogens are ordered in a manner that prevents the rotation of polarized light or that a thin film of LCP_{OMe}, unlike in bulk, does not contain enough mesogens to rotate light. However, in films where the last LCP_{OMe} layer was not confined by PEN on the top, i.e., the topmost SCLCP layer was in contact with air, a pattern was visible with POM. It was observed around 140 °C, before the films reached T_{iso}, droplets started forming. It was these droplets that exhibited LC behavior similar to bulk as shown in Figure 22. This

characteristic LC behavior in POM, however, was only observed when cooling the films at 0.2 °C/min.

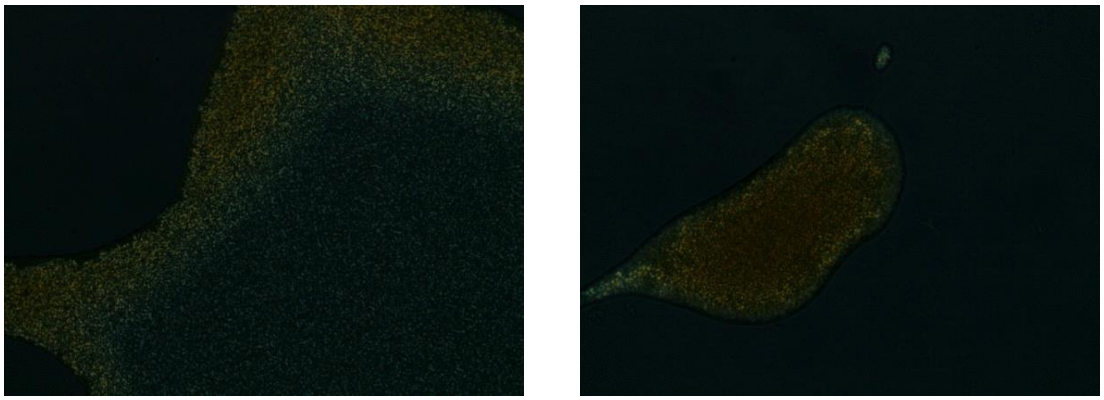

Figure 22. POM images of 300 nm SCLCP layers in a 4-layer film (no top confining PEN layer) showing the LC behavior in droplets when cooling at 0.2 °C/min.

This phenomenon, present in films without a topmost confining layer, can be attributed to dewetting processes of the topmost SCLCP layer. It can be concluded that the SCLCP layer thickness of 300 nm in as cast samples without PEN as the topmost layer are not thick enough to enable the detection of light rotation, that is, there might not be enough mesogens stacked in order to show birefringence. Once the droplets form from dewetting processes, the SCLCP layer thickness in these areas is thicker allowing more mesogens to stack up leading to the appearance of birefringence. Likewise, when the LCP_{OMe} is confined on both sides by PEN (T_g = 180 °C), the SCLCP is confined to 300 nm thickness at all temperatures below 180 °C, thus no LC behavior can be observed. The same features were observed in films with a LCP_{OMe} layer thickness of 800 nm. The fact that polarized light is not rotated is a confinement effect for these materials. It is unclear what threshold SCLCP thickness these effects begin, but it is presumably greater than 800 nm.

WAXD studies of as-cast multilayered films on glass substrates showed no peaks, meaning the as-cast films have no defined order. This also prevented the assignment of the LC mesophase type. Yet, these results are not surprising given the seeming lack of ordering detected by POM for SCLCP when confined by PEN on both sides, and the previous WAXD results of LCP_{OMe} in bulk, which lacked any distinct LC peaks.

Lastly, the as-cast films were studied by polarized UV-Vis spectroscopy. When conducting the as-cast UV-Vis spectroscopy experiments, it was noticed that the absorption of the films was beyond the equipment limits. In order to avoid erroneous data, films were made with 3 layers (one 300 nm-thick LCP layer), 7 layers (three 100 nm-thick LCP layers), and 6 layers (three 50 nm-thick LCP layers). It has been shown [33] that the order parameter of LCPs, *S*, can be obtained from

$$S = \frac{A_{\parallel} - A_{\perp}}{A_{\parallel} + 2A_{\perp}}$$

where $A_{\parallel}$represents the maximum absorbance in the spectra when the polarizer is parallel to the reference direction, and $A_{\perp}$ represents the maximum absorbance in the spectra when the polarizer is perpendicular to the reference direction. Following this procedure it was found that the as-cast films, regardless of thickness, do not have any preferential order and have order parameters in the range of 0.0011 to 0.0247, with the film containing the 300 nm-thick SCLCP layer having the greatest *S*. It can be concluded that confinement alone does not induce ordering.

Alignment

A known method for developing ordering of azobenzene SCLCPs in a predisposed direction is through irradiation with light. The multilayered films in this study were aligned by this method after as-cast characterization. First, the films were photoaligned by exposure to 4500 mJ/cm^2 of unpolarized UV light (365 nm wavelength)

followed by exposure to 720 mJ/cm^2 of polarized visible light (450 nm wavelength) as delineated in literature[33]. All films were marked before alignment to define the reference direction. The use of unpolarized UV light will help the SCLCP reach a state with the highest content of mesogen *cis* isomers which disorders the mesophase, while the use of polarized visible light will promote mesogen *trans* isomers and induce orientation of the azobenzene groups in the direction perpendicular to the polarization of the light. The photoalignment was performed at a temperature 15 °C above T_g to allow the polymer to have mobility to adjust to photoalignment conditions.

After the films were photoaligned and characterized, the films were then thermally annealed at a temperature in the ΔT_{LC} range (T = 130 °C; T_g = 96 °C; T_{iso} = 147 °C) for 3 days under vacuum. In order to prevent the loss of photoaligned order, the films were kept in the dark during annealing. The films were then cooled slowly (about 0.2 °C/min) through the T_g transition while under vacuum so that ordering could develop.

Aligned Characterization

Multilayered films were characterized immediately after photoalignment and after thermal annealing following photoalignment. All characterization of the multilayered films was conducted in the dark to avoid any further photoisomerization or loss of alignment.

WAXD spectra of the multilayered films with a topmost PEN confining layer are presented in Figure 23. When the WAXD experiments were performed on any of the films as-cast, there is no peak present. After both photoaligning, and photoalignment followed by thermal annealing, films with a LCP_{OMe} layer thickness of 50 and 100 nm developed a sharp peak around $2\theta = 4.9°$, which corresponds to a d-spacing of 18 Å according to Bragg's law. Theoretically this d-spacing corresponds to a Smectic A

mesophase arrangement where the side chains from different polymer chains are intercalated, fully overlapping, and the polymer backbone is unaffected by the mesogen ordering[31]. However, this is not the case for films with LCP layer thicknesses of 300 nm and 800 nm. Films containing LCP_{OMe} layer thicknesses of 300 nm showed a sharp peak at $2\theta = 3.5°$ only after thermal annealing, which corresponds to a d-spacing of approximately 25 Å. This d-spacing, on the other hand, corresponds to a Smectic A mesophase arrangement where the mesogens from different polymer chains are intercalated, side by side, and the polymer backbone is unaffected by the mesogen ordering[31]. In the case of the film containing an 800 nm-thick LCP_{OMe} layer, a peak at $2\theta = 4.9°$ is only seen after thermal annealing. This peak coincides with the Smectic A arrangement first described. While the WAXD results on the films with LCP layer thicknesses of 50 and 100 nm are expected (i.e., the appearance of a characteristic LC peak after alignment), the WAXD results on the films with LCP later thicknesses of 300 and 800 nm are puzzling. The lack of a peak in these films after photoalignment could possibly be due to the LCP_{OMe} layers being too thick for the polarized light to penetrate and isomerize the mesogens. It is only after thermal annealing, which can equally penetrate all layers regardless of thickness that an ordering peak appears. Yet, the film containing the LCP layer thickness of 300 nm exhibits a peak at a completely different scattering angle. A possible explanation for this phenomenon is that confinement of the LCP_{OMe} to 300 nm causes the mesogens and polymer backbone to arrange differently because the thickness allows the polymer backbone to move and arrange itself in between mesogen stacks of about 18.7 Å. A thickness of 50 or 100 nm might be too small to allow the polymer backbone to be secluded in between mesogen stacks, while a thickness of 800 nm might be too thick to affect the polymer backbone, thus allowing the backbone to be in an isotropic state at this thickness.

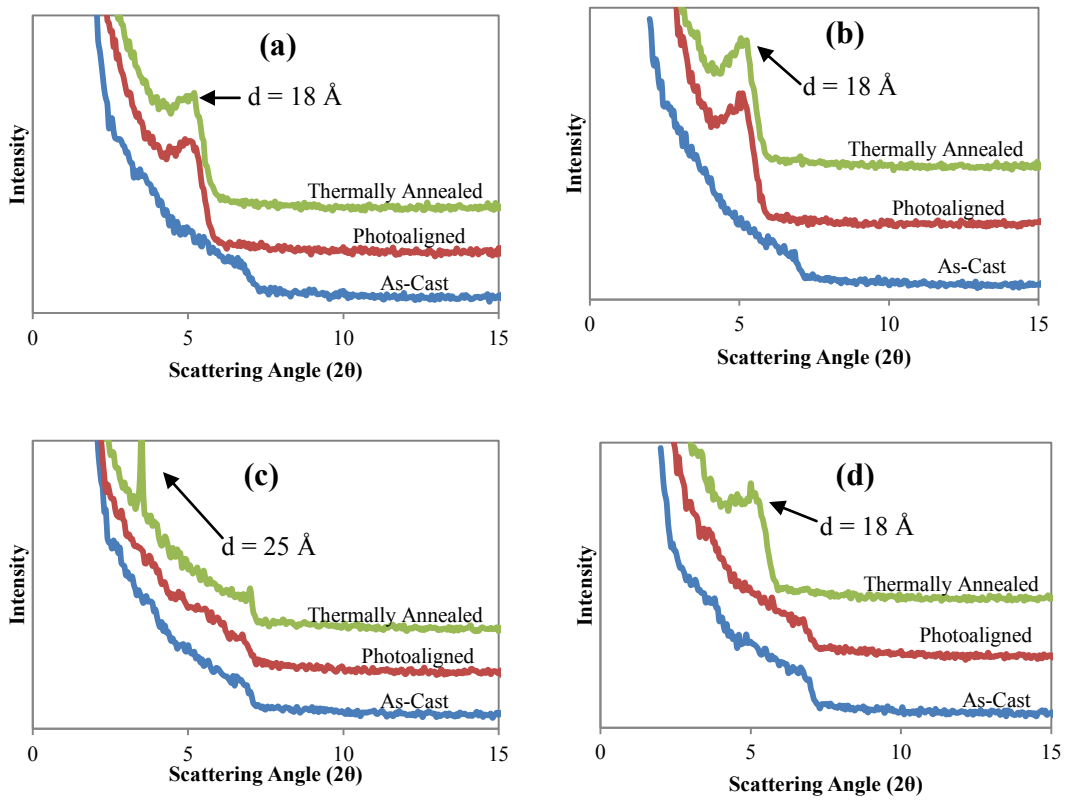

Figure 23. WAXD spectra for multilayered films with LCP_{OMe} layer thicknesses of (a) 50 nm, (b) 100 nm, (c) 300 nm and (d) 800 nm as-cast, after photoalignment, and after thermally annealing following photoalignment. All films presented here had a topmost PEN confining layer.

Using multilayered films with a topmost confining PEN layer when the SCLCP layer was 100, 300 or 800 nm thick (i.e., the film with 50 nm-thick LCP layers was not confined on the top with PEN), the polarized UV-Vis spectra was employed to determine the order parameter, *S*, of the LCP layers. A sample of polarized UV-Vis spectra is shown in Figure 24. Figure 25 presents the *S* of the multilayered films both as a function of film thickness and of treatment. While the *S* of the as-cast films is close to 0 (isotropic), the *S* of the films following photoalignment at a temperature above the T_g is in the range of

0.149 to 0.25. In the case of the multilayered films that were thermally annealed following the photoalignment, the *S* values range from 0 to 0.056. The decrease in *S* in photoaligned samples after thermal annealing could be due to a change in preferential ordering direction. While photoalignment encourages the alignment of mesogens in the direction perpendicular to the light polarization since there is no light absorption there[34], thermally annealing allows the mesogens to align in their preferential direction defined by the mesogen chemistry, spacer length and polymer backbone flexibility[7].

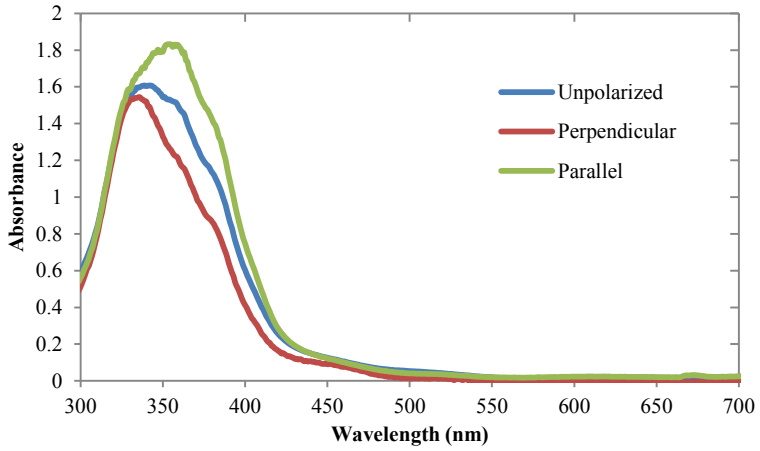

Figure 24. Sample polarized UV-Vis spectra of films containing 100 nm-thick LCP layers after photoalignment above T_g.

After alignment, the multilayered film containing the 50 nm–thick LCP layers had the greatest *S* value. Isomerization to *cis* isomers can cause expansion of the irradiated layer[34]. Because the multilayer film with the 50 nm-thick LCP layer has no PEN confining layer on the top (addition of this last layer compromises the layer quality as described in the materials section), the topmost LCP layer is free to photoisomerize and expand allowing the layer to order itself. This may explain why this film has a higher *S* value when thermally annealed. Unfortunately, since the *S* from polarized UV-Vis studies

is an average of the order parameter of each individual layer, at this time we are unable to determine if this *S* is representative of all the layers or if it corresponds to the average of a top layer with an individual high *S* and other layers with individual low *S*.

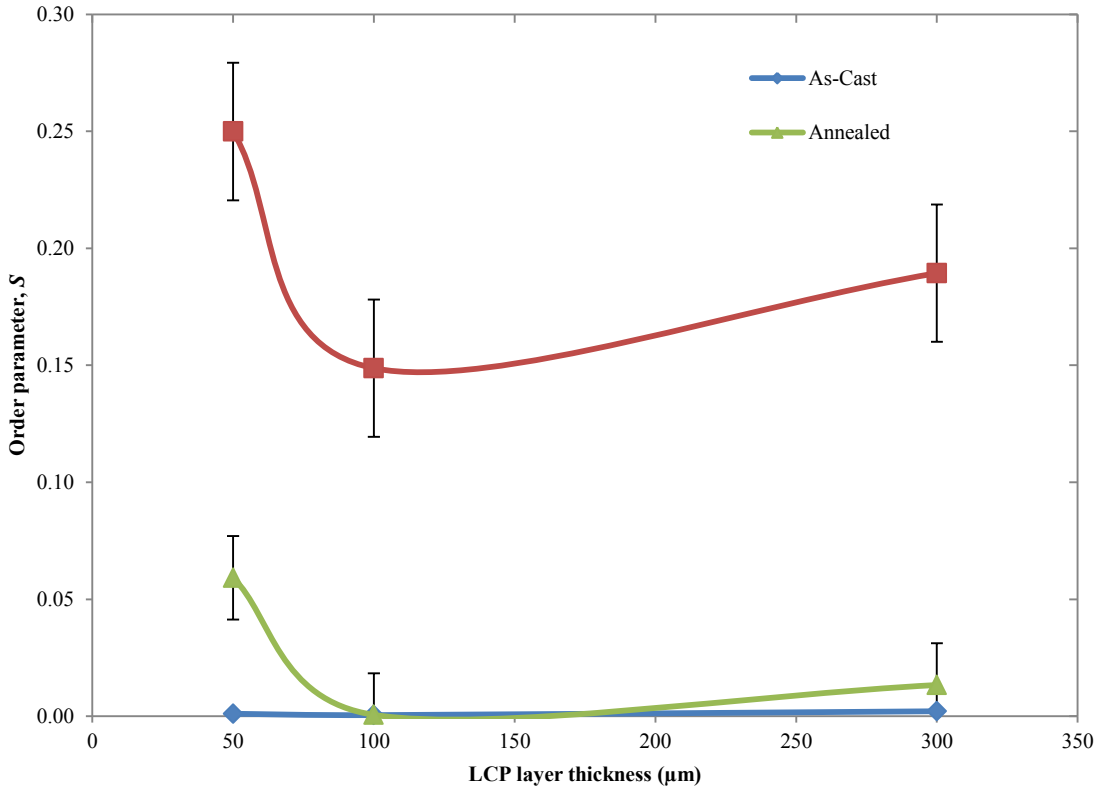

Figure 25. Order parameter, *S*, of multilayered films as a function of LCP layer thickness. It should be noted that films with LCP_{OMe} layer thicknesses of 100 and 300 nm had a topmost confining layer while the film with LCP_{OMe} layer thickness of 50 nm did not have a topmost confining layer.

On the other hand, the fact that the multilayer film containing the 100 nm-thick LCP layer was the lowest when compared to the multilayer film containing the 300 nm-thick LCP layer in both the photoaligned and thermally annealed cases might be attributed to anchoring effects in thinner layers. Anchoring effects are caused by

interactions between the LC mesogens and the confining polymer which prevent the mesogens closest to the interfaces from aligning with the rest of the mesogens in the layer. This effect has been reported in SCLCPs confined within block copolymer microdomains[33].

Conclusion

SUMMARY OF FINDINGS

In the course of this project we were able to successfully modify a commercially-available MCLCP, study the effects of confinement on the ordering of SCLCPs, and explored the possibility of making HBLCPs based on commercially-available polymer backbones and mesogens with properties that would allow melt processing of the samples.

MCLCP Vectra was melt mixed with 4 wt% TPP for 30 min resulting in a 20 fold increase in viscosity while maintaining its LC behavior. However, if 5 wt% TPP was added, the viscosity didn't increase as much, possibly due to an equilibrium shift in the chain coupling reactions. Combustion as well as FTIR analysis corroborated the presence of phosphorus in the polymer chains, supporting the proposal that the phosphorus acts as a link between Vectra polymer chains effectively increasing their molecular weight and as a result, their viscosity. Unfortunately, the viscosity of Vectra-TPP 4% was reduced to that of neat Vectra when the Vectra-TPP samples were reprocessed under an air atmosphere, similar to how they would be processed into film.

After exploring several possibilities for HBLCPs, it was found that those based on ionomers are the best option for obtaining the thermal and rheological properties required for melt processing into films. However, these LCIs showed significant weight loss above 167 °C from mesogen degradation, which could be resolved by changing the mesogen. Inconclusive WAXD and POM studies prevented us from determining whether the material forms a continuous LC phase or small LC microdomains confined only to the ionomer clusters as has been proposed in literature.

LCP_{OMe} SCLCP was successfully synthesized and confined into multilayered films using PEN as a confining layer. Films were made with varying LCP layer

thicknesses and total numbers of layers. Confinement of LCP_{OMe} by PEN on both interfaces did not allow the LCP layer to rotate light when observed under POM. When the top PEN confining layer was removed, the topmost LCP layer dewet and exhibited bulk-like LC optical behavior under POM. The domains present in the POM studies, both in bulk and after dewetting of the SCLCP surface layer, were not large enough to assign a mesophase type. WAXD studies of the bulk LCP_{OMe} and as-cast multilayered films showed no distinct peaks. On the other hand, WAXD spectra of multilayered films showed a sharp peak corresponding to a d-spacing of 18 Å after photoalignment and thermal annealing for samples with LCP layer thicknesses of 50 and 100 nm. Samples with LCP layer thicknesses of 300 and 800 nm presented peaks only after thermal annealing corresponding to a d-spacing of 25 and 18 Å, respectively. The peak in films of LCP thicknesses of 50, 100 and 800 nm fits with a model of a Smectic A mesophase where the mesogens of different polymer chains are intercalated side by side while the polymer backbone remains unaffected by the mesogen ordering. Multilayered films with LCP thickness layer of 300 nm presented a peak at a different scattering angle, which agrees with a different Smectic A arrangement model.

Polarized UV-Vis studies were used to determine the order parameter, *S*, of the films. Since the measured *S* is an average of the order in all the layers, we were unable to determine if the resulting *S* corresponds to equal ordering in all the layers or only a high degree of order in the top-most layer. *S* values were greater when the films were photoaligned at temperatures above the T_g of the SCLCP. The multilayered film with 50 nm-thick LCP layer had the biggest *S* value both after photoalignment and thermal annealing since there was no top PEN confining layer, which allowed the LCP to isomerize and expand as needed. It was also observed that the films containing 100 nm-

thick LCP layers had the lowest *S* values, possibly due to anchoring effects. It could be predicted that a higher *S* would correlate to improved properties for use as a gas barrier.

PROPOSED FUTURE WORK

To make a HBLCP with the thermal and rheological properties necessary for melt processing, commercial polyvinylidene fluoride (PVDF) could be mixed with a high-boiling commercial LC mesogen to produce an LCP with hydrogen bonds (-C-H···F-) that are stronger than those in the LCIs previously studied. PVDF has also been previously coextruded so the viscosity of the HBLCP might not be an issue. Figure 26 shows the POM of a preliminary mixture of PVDF with azobenzene-containing NMe.

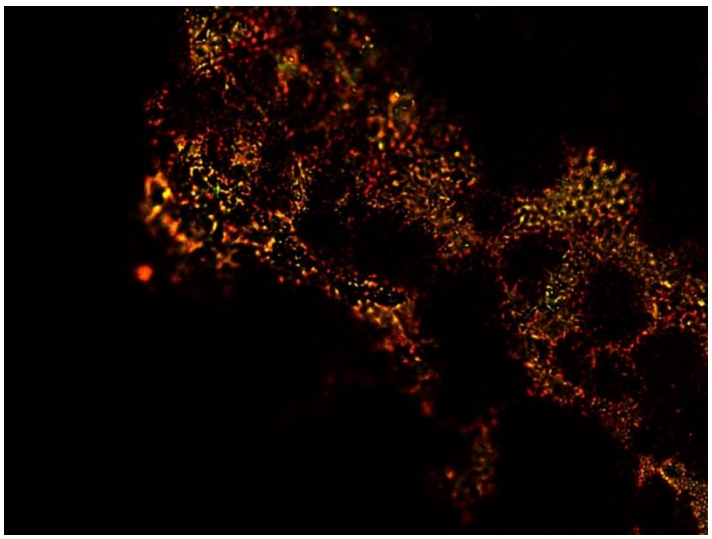

Figure 26. POM image of PVDF with mesogen LC_{NMe} in a 1:1 molar ratio (two LC molecules per PVDF repeat unit; approximately 13 wt% LC).

Confinement studies showed that multilayer films with a topmost confining layer and 100 nm-thick LCP layers were more susceptible to anchoring effects, while films with 300 nm-thick LCP layers could be treated to induce ordering. Future work should

determine whether the *S* values determined by polarized UV-Vis studies are due to a highly ordered topmost LCP layer with less ordered bottom layers or due to equally ordered LCP layers throughout the multilayered films. The polarized UV-Vis spectra of multilayered films with the same LCP layer thickness, but varying number of layers could be used for this purpose. If the *S* of all these multilayered films remains unchanged then it can be concluded that the *S* calculated from polarized UV-Vis experiments corresponds to the average of equally ordered LCP layers throughout the film. On the other hand, if the *S* decreases with an increase in number of layers, it can be concluded that the *S* calculated from polarized UV-Vis experiments corresponds to the average of a highly ordered top LCP layer with bottom LCP layers with lower order. The multilayer films that show the greatest *S* values after alignment can then be tested to determine if enhanced ordering changes crystallization, optical, mechanical and barrier properties, among others.

Given the inability to melt process LCP_{OMe}, changes could be made to the structure to improve its viscosity. Making the LCP homopolymer into a diblock or triblock once again with a non-glassy end block might provide the structure necessary to increase the viscosity, yet allow the final SCLCP to flow with suitable viscosity at high temperatures. Likewise, changing the backbone of the homopolymer from a PS based one could also increase the rigidity of the polymer chains and thus increase the viscosity of the homopolymer. Another option is to change the LC spacer length, which has been shown to have a direct effect on the rheological properties of SCLCPs[35] .

References

(1) Wang, H.; Keum, J. K.; Hiltner, A.; Baer, E.; Freeman, B.; Rozanski, A.; Galeski, A. *Science* **2009**, *323*, 757-760.
(2) Park, J. Y.; Paul, D. R.; Haider, I.; Jaffe, M. *J. Polym. Sci.: Polym. Phys.* **1996**, *34*, 1741-1745.
(3) Liu, R. Y. F.; Ranade, A. P.; Wang, H. P.; Bernal-Lara, T. E.; Hiltner, A.; Baer, E. *Macromol.* **2005**, *38*, 10721-10727.
(4) Mackey, M.; Flandin, L.; Hiltner, A.; Baer, E. *J. Polym. Sci.: Polym. Phys.* **2011**, *49*, 1750-1761.
(5) Ponting, M.; Hiltner, A.; Baer, E. *Macromol. Symp.* **2010**, *294-I*, 19-32.
(6) Ponting, M.; Lin, Y. J.; Keum, J. K.; Hiltner, A.; Baer, E. *Macromol.* **2010**, *43*, 8619-8627.
(7) Wang, X.; Zhou, Q. *Liquid crystalline polymers*; World Scientific Pub. Co.: River Edge, N.J., 2004.
(8) Pebalk, D. A.; Barmatov, E. B.; Shibayev, V. P. *Russ. Chem. Rev.* **2005**, *74*, 610-633.
(9) Constant, D. R. In *Paper, Film & Foil Converter*, 2002.
(10) Lusignea, R. *P Tech as P* **1996**, 115-124.
(11) Loth, H.; Euschen, A. *Makromol. Chem.-Rapid* **1988**, *9*, 35-38.
(12) Kato, T.; Mizoshita, N.; Kanie, K. *Macromol. Rapid Commun.* **2001**, *22*, 797-814.
(13) Armstrong, G.; Buggy, M. *J Mater Sci* **2005**, *40*, 547-559.
(14) Gayathri, K.; Balamurugan, S.; Kannan, P. *J Chem Sci* **2011**, *123*, 255-263.
(15) Crivello, J. V.; Deptolla, M.; Ringsdorf, H. *Liq. Cryst.* **1988**, *3*, 235-247.
(16) Petr, M.; Hammond, P. T. *Macromol.* **2011**, *44*, 8880-8885.
(17) Odian, G. G. *Principles of polymerization*; 4th ed.; Wiley-Interscience: Hoboken, N.J., 2004.
(18) Jannasch, P. *Macromol.* **2000**, *33*, 8604-8610.
(19) Borkar, S. Dissertation, University of Duisburg-Essen, 2003.
(20) Aharoni, S. M. *Polym. Bull.* **1983**, *10*, 210-214.
(21) Aharoni, S. M. *Int. J. Polymer. Mater.* **1994**, *26*, 9-17.
(22) Aharoni, S. M.; Forbes, C. E.; Hammond, W. B.; Hindenlang, D. M.; Mares, F.; Obrien, K.; Sedgwick, R. D. *Journal of Polymer Science Part a-Polymer Chemistry* **1986**, *24*, 1281-1296.
(23) Aharoni, S. M.; Hammond, W. B.; Szobota, J. S.; Masilamani, D. *Journal of Polymer Science Part a-Polymer Chemistry* **1984**, *22*, 2567-2577.
(24) Cavalcanti, F. N.; Teofilo, E. T.; Rabello, M. S.; Silva, S. M. L. *Polym. Eng. Sci.* **2007**, *47*, 2155-2163.
(25) Jacques, B.; Devaux, J.; Legras, R.; Nield, E. *Polymer* **1996**, *37*, 1189-1200.
(26) Jacques, B.; Devaux, J.; Legras, R.; Nield, E. *Polymer* **1997**, *38*, 5367-5377.
(27) Jacques, B.; Legras, R.; Devaux, J.; Nield, E. *Makromolekulare Chemie-Macromolecular Symposia* **1993**, *75*, 231-236.

(28) Eisenberg, A.; Kim, J.-S. *Introduction to ionomers*; Wiley: New York, 1998.
(29) Martinez-Felipe, A. *Liq. Cryst.* **2011**, *38*, 1607-1626.
(30) Li, Z. P.; Garza, P. A. G.; Baer, E.; Ellison, C. J. *Polymer* **2012**, *53*, 3245-3252.
(31) Imrie, C. T.; Schleeh, T.; Karasz, F. E.; Attard, G. S. *Macromol.* **1993**, *26*, 539-544.
(32) Imrie, C. T.; Karasz, F. E.; Attard, G. S. *Liq. Cryst.* **1991**, *9*, 47-57.
(33) Tong, X.; Cui, L.; Zhao, Y. *Macromol.* **2004**, *37*, 3101-3112.
(34) Zhao, Y.; Ikeda, T. *Smart light-responsive materials : azobenzene-containing polymers and liquid crystals*; Wiley: Hoboken, N.J., 2009.
(35) Lee, K. M.; Han, C. D. *Macromol.* **2003**, *36*, 8796-8810.

Vita

Paola A. Gonzalez Garza was born in Miguel Alemán, Tamaulipas, México. She lived in Saltillo, Coahuila, México during all of her childhood and her early teens. After completing her work at The Science Academy of South Texas, Mercedes, Texas, in 2005, she entered The University of Texas – Pan American (UTPA) in Edinburg, Texas. She received the degree of Bachelor of Science in Mechanical Engineering and Chemistry from UTPA in August 2009. In August of that same year, she entered the Graduate School at The University of Texas at Austin.

Email Address: paola.gonzz@gmail.com

This thesis was typed by Paola Anaid González Garza.